Letter

Unraveling higher-order contributions to spin excitations probed using resonant inelastic x-ray scattering

Umesh Kumar , 1,* Abhishek Nag, 2,† Jiemin Li, 2,3 H. C. Robarts, 2,4 A. C. Walters , 2 Mirian García-Fernández , 2 R. Saint-Martin , 5 A. Revcolevschi, 5 Justine Schlappa, 6 Thorsten Schmitt, 7 Steven Johnston, 8,9 and Ke-Jin Zhou , 2,‡

1 Theoretical Division, Los Alamos National Laboratory, Los Alamos, New Mexico 87545, USA

2 Diamond Light Source, Harwell Campus, Didcot OX11 ODE, United Kingdom

3 Beijing National Laboratory for Condensed Matter Physics and Institute of Physics, Chinese Academy of Sciences, Beijing 100190, China

4 H. H. Wills Physics Laboratory, University of Bristol, Bristol BS8 ITL, United Kingdom

5 Institut de Chimie Moléculaire et des Matériaux d'Orsay, Université Paris-Saclay, UMR 8182, 91405 Orsay, France

6 European X-Ray Free-Electron Laser Facility GmbH, Holzkoppel 4, 22869 Schenefeld, Germany

7 Photon Science Division, Paul Scherrer Institut, 5232 Villigen PSI, Switzerland
8 Department of Physics and Astronomy, The University of Tennessee, Knoxville, Tennessee 37996, USA

9 Institute for Advanced Materials and Manufacturing, University of Tennessee, Knoxville, Tennessee 37996, USA



(Received 24 September 2021; revised 17 January 2022; accepted 3 August 2022; published 18 August 2022)

Resonant inelastic x-ray scattering (RIXS) is an evolving tool for investigating the spin dynamics of strongly correlated materials, which complements inelastic neutron scattering. In isotropic spin- $\frac{1}{2}$ Heisenberg antiferromagnetic (HAFM) spin chains, both techniques have observed non-spin-conserving (NSC) excitations confined to the two-spinon phase space. However, a recent O K-edge RIXS study of the one-dimensional HAFM Sr_2CuO_3 observed spin-conserving (SC) four-spinon excitations outside the two-spinon phase space. Here, we demonstrate that analogous four-spinon excitations can also be accessed at the CuL_3 edge in the related material $SrCuO_2$. Through detailed modeling, we establish that these excitations appear in both the SC and NSC channels of the CuL_3 edge, and are only captured by higher-order terms in the ultrashort core-hole lifetime expansion. Since these terms encode information about spin-spin correlations extending beyond nearest neighbors, our results offer different possibilities for studying nonlocal spin correlations in quantum magnets.

DOI: 10.1103/PhysRevB.106.L060406

The elementary excitations of a system encode information about the microscopic origin of its behavior. For example, magnetic excitations are extensively studied in high- T_c superconducting cuprates for their possible role in the pairing mechanism and provide access to critical physical parameters such as their correlation strength, superexchange interactions, and electronic structure parameters [1–7]. Inelastic neutron scattering (INS) has traditionally been the method of choice for probing magnetic correlations. In recent years, however, resonant inelastic x-ray scattering (RIXS) has emerged as an important complementary technique [8–19]. Its large scattering cross section and element specificity are advantageous over INS for small sample volumes, as well as for complex systems with multiple magnetic elements [20,21].

While the relationship between the INS cross section and the dynamical spin structure factor $S(\mathbf{q}, \omega)$ is well understood, the same cannot be said about the RIXS cross section, which is described by the Kramers-Heisenberg (KH) formalism [8]. The RIXS intensity can only be directly equated with dynamical structure factors under certain scattering conditions [22] or in the limit of an ultrashort core-hole lifetime

(UCL) [23], a fact that is becoming more evident with the recent developments in resolving the polarization of scattered x rays [11,24,25]. Moreover, the elemental sensitivity of RIXS means that one needs to account for the details of the edge to understand its spectra. For example, for copper oxide materials, only spin-conserving excitations are allowed at the oxygen (O) K edge while both spin-conserving (SC, $\Delta S_{\text{tot}} = 0$) and non-spin-conserving (NSC, $\Delta S_{\text{tot}} = 1$) excitations are allowed at the copper (Cu) L edge.

These aspects complicate the interpretation of RIXS experiments; however, they have also led to the observation of novel excitations [26–31]. For example, SC four-spinon excitations have recently been observed outside the two-spinon continuum [28,29] in the one-dimensional (1D) isotropic Heisenberg antiferromagnetic (HAFM) spin chain Sr₂CuO₃. Before this, INS studies had only uncovered four-spinon excitations outside of the two-spinon phase space in materials with frustrated magnetic interactions [32] or long-range interorbital hopping [33]. In contrast, for isotropic 1D HAFMs, INS has only been able to infer the presence of four-spinon excitations within the two-spinon continuum through precise measurements of the spectral weight of $S(q, \omega)$ [34,35]. O K-edge RIXS, on the other hand, observes such excitations directly because of the finite lifetime of the O 1s core hole, which enables long-range double spin flips in the system. This observation thus provides another tool for directly

^{*}umesh.kumar@rutgers.edu

[†]abhishek.nag@diamond.ac.uk

[‡]kejin.zhou@diamond.ac.uk

accessing long-range spin dynamics in quantum materials. Its utility, however, would be greater if similar effects could be demonstrated at the shorter-lived transition metal L edges, as it is richer and the UCL approximation is justifiable at this edge [22,23].

In this Letter, we study the spin dynamics of the 1D HAFM SrCuO₂ with high-resolution Cu L₃- and O K-edge RIXS. We observe excitations in the two-spinon continuum, in agreement with INS on this system [36]. However, we also observe considerable spectral weight from four-spinon excitations outside of the two-spinon continuum, but with distinct distributions of spectral weight at each edge. The four-spinon excitations observed at the O K edge appear in the SC channel, as reported in a related work on Sr₂CuO₃ [28]. Using detailed theoretical modeling within the KH formalism for the t-J model, we demonstrate that the four-spinon excitations observed in the Cu L_3 -edge spectra appear in both SC and NSC scattering channels. We further evaluate other dynamical correlation functions derived from the UCL expansion to show that these four-spinon excitations can only be accounted for by higher-order terms of the expansion involving long-range spin-spin correlations. These observations further demonstrate the utility of RIXS for studying magnetic correlations in quantum materials.

SrCuO₂ contains edge-shared CuO₄ plaquettes arranged in a zigzag geometry with negligible interchain coupling [Fig. 1(a)] [36–41]. The Cu sites have $3d^9$ valence configurations in the atomic limit with a hole in the $d_{x^2-y^2}$ orbital. Due to strong intrachain coupling, the system effectively behaves as a 1D spin- $\frac{1}{2}$ HAFM chain above $T_N = 5$ K [36,41]. The zigzag arrangement of the plaquettes creates two inequivalent oxygen sites denoted O_A and O_B , as shown in Fig. 1(a). Due to the element specificity of the RIXS process, excitations of the in-chain O_B or Cu sites can be isolated by fixing the incident energy to x-ray absorption spectra (XAS) peaks from these respective elements. We obtained the resonant energies of the O_B and Cu sites from the XAS collected at the O K (resonance at \sim 529.8 eV) and Cu L_3 (resonance at ~931.8 eV) edges, respectively [see Supplemental Material (SM) Fig. S1] [40,42]. RIXS spectra on SrCuO₂ at 13 K were collected at the O K and Cu L_3 edges with energy resolutions of ~27 and ~42 meV, respectively, at I21 beamline, Diamond Light Source, U.K. [43]. Throughout, the momentum transfer component along the chain direction (q_{\parallel}) is presented in units of $2\pi/b$.

Figures 1(b) and 1(c) show the RIXS spectra from SrCuO₂ for $q_{\parallel}=0.175$ at the Cu L_3 and O K edges, respectively. Similar to RIXS results on the related compound Sr₂CuO₃, phonon excitations and their overtones are observed below ~ 0.2 eV for both edges [26,28]. The intense feature close to 0.35 eV energy loss at the Cu L_3 edge can be ascribed to a two-spinon excitation and approximated by the dynamical structure factor computed using the Müller ansatz after, adopting an exchange coupling J=0.225 eV [36,44]. A weaker feature is also observed at the O K edge at a similar energy. Figures 1(d) and 1(e) show the RIXS spectra for $q_{\parallel}=0.0$ at the Cu L_3 and O K edges, respectively. For both edges, significant spectral weight is observed, peaking close to 0.5 eV. Since the weight of the two-spinon continuum is zero at this momentum point, and the orbital and charge-transfer

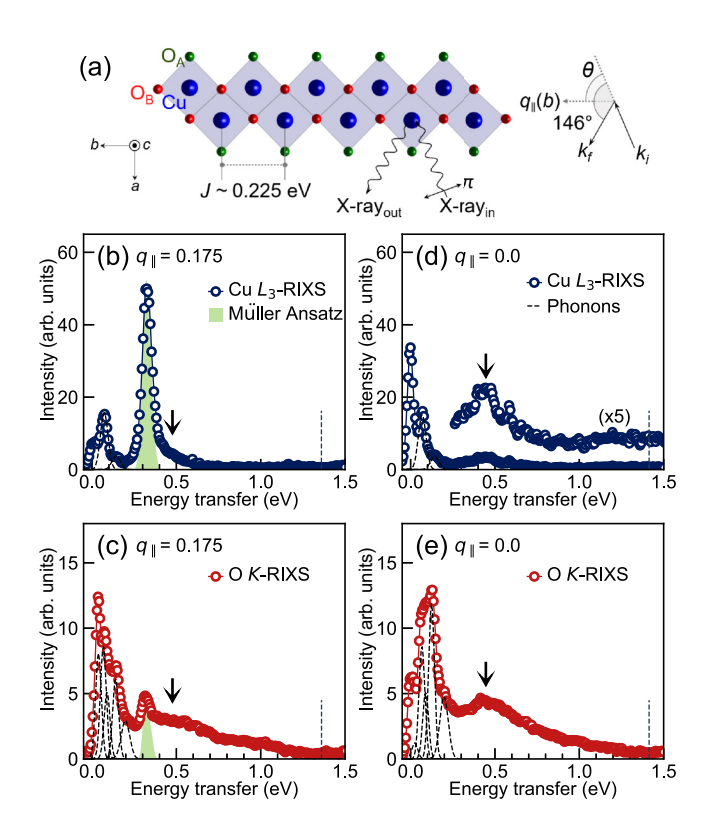


FIG. 1. (a) A schematic diagram of the RIXS scattering geometry for $SrCuO_2$. (b) and (c) show the low-energy $Cu\ L_3$ - and $O\ K$ -edge RIXS spectra, respectively, measured at $q_{\parallel}=0.175$. (d) and (e) show the corresponding data at $q_{\parallel}=0$. Also shown in (d) is the RIXS spectrum multiplied by a factor of five and vertically shifted. At $q_{\parallel}=0$, the energy of the two-spinon excitations and their spectral weight are zero. For $q_{\parallel}=0.175$, the two-spinons are approximated by the Müller ansatz [44]. The vertical dashed line indicates the upper boundary of the four-spinon continuum [45]. In all cases, additional spectral weight (marked by arrows) is observed outside the two-spinon phase space but inside the four-spinon phase space.

excitations lie above 1.5 eV, these features likely arise from four-spinon excitations [28]. Overall, it appears that RIXS probes similar excitations at both edges but with substantially different scattering cross sections, giving rise to distinct spectral weight distributions. For a better understanding of the RIXS cross sections, we next map these excitations in the energy-momentum space.

Figures 2(a) and 2(b) present the momentum-resolved RIXS intensity maps at the O K and Cu L_3 edges, respectively. The lower and upper boundaries of the two-spinon phase space, $\omega_{2S}^1(\mathbf{q}) = \frac{\pi}{2}J|\sin(qb)|$ and $\omega_{2S}^u(\mathbf{q}) = \pi J|\sin(qb/2)|$ [44], are plotted over the maps for J=0.225 eV. A highly dispersing spectral weight is observed within this phase space, consistent with INS experiments on SrCuO₂ [36]. The two-spinon continuum composed of fractionalized spin- $\frac{1}{2}$ entities has been previously observed at Cu L_3 -edge RIXS for Sr₂CuO₃, Ca₂CuO₃, and CaCu₂O₃ [26,28,46,47], where they arise from a spin-flip scattering process enabled by the strong spin-orbit coupling in the 2p core level. In O K-edge RIXS, where a single spin flip is not allowed, two-spinon excitations are created by a net

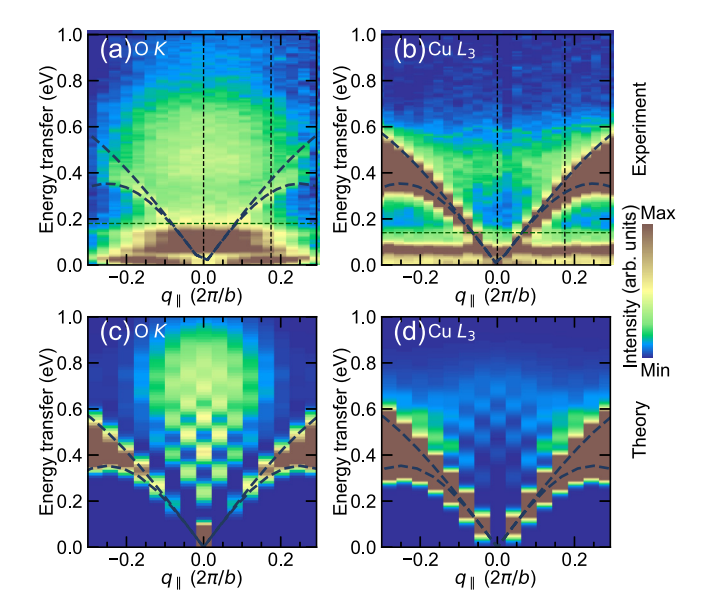


FIG. 2. (a) O K-edge and (b) Cu L_3 -edge RIXS intensity maps for momentum transfer along the chain. The brown color represents the maximum spectral weight in the color scale. The two-spinon continuum boundaries are shown by blue dashed lines. Horizontal dashed green lines mark the higher-energy limit of the phonon excitations. The RIXS spectra shown in Figs. 1(b)-1(e) correspond to the vertical black dashed lines. Model intensity maps for spin excitations at the (c) O K edge and (d) Cu L_3 edge computed using the Kramers-Heisenberg formalism.

spin-zero nearest-neighbor double spin-flip process [28,48]. Further, due to the longer core-hole lifetime at the O K edge, quantum fluctuations lead to the formation of additional domain walls in the intermediate state [28]. Four-spinon excitations are thus formed, appearing as an additional continuum of excitations located outside the two-spinon phase space [Fig. 2(a)] but within the four-spinon phase space extending up to $\omega_{4S}^{u}(\mathbf{q}) = \pi J \sqrt{2[1+\cos(qb/2)]}$ (\sim 1.4 eV for J=0.225 close to $g_{\parallel}=0$) [45].

Interestingly, we also observe significant spectral weight outside the two-spinon phase space in Cu L_3 -edge measurements. Similar features were reported by Ref. [28], but were not explored further. Notably, the four-spinon spectral weight distributions are drastically different between the two edges for the same system. While they form a bulbous shape with the largest weight close to $q_{\parallel}=0$ at the O K edge, they have a flatter distribution with weight collected near the upper boundary of the two-spinon continuum at the Cu L_3 edge.

The low-energy spin dynamics of corner-shared cuprates are well described by the t-J Hamiltonian [28,36,49–51]

$$H = -t \sum_{\langle i,j \rangle,\sigma} \tilde{c}_{i,\sigma}^{\dagger} \tilde{c}_{j,\sigma} + J \sum_{i} \left(\mathbf{S}_{i} \cdot \mathbf{S}_{i+1} - \frac{1}{4} n_{i} n_{i+1} \right). \quad (1)$$

Here, t and J are the hopping integral and exchange coupling, respectively, between nearest neighbors $\langle i,j\rangle$; $\tilde{c}_{i,\sigma}^{\dagger}$ ($\tilde{c}_{i,\sigma}$) is the creation (annihilation) operator for a spin- σ (= \uparrow , \downarrow) hole at site i under the constraint of no double occupancy; $n_i = \sum_{\sigma} \tilde{c}_{i,\sigma}^{\dagger} \tilde{c}_{j,\sigma}$ is the number operator; and \mathbf{S}_i is the spin operator at site i. We use J = 0.225 eV from the energy-

momentum distribution of the two-spinon continuum in our RIXS experiments and t = 0.3 eV, typical for cuprates.

We solved Eq. (1) on 24 site chains using exact diagonalization (ED) and evaluated the RIXS intensity $I(q, \omega)$ using the KH formalism [8],

$$I(q,\omega) \propto \sum_{f} \left| \sum_{n} \frac{\langle f | D_{k_{\text{out}}}^{\dagger} | n \rangle \langle n | D_{k_{\text{in}}} | g \rangle}{E_{g} + \omega_{\text{in}} - E_{n} + i \Gamma_{n}} \right|^{2} \delta(E_{f} - E_{g} - \omega).$$
 (2

In the above expression, the incoming (outgoing) photons have energy $\omega_{\rm in}$ ($\omega_{\rm out}$) and momentum $k_{\rm in}$ ($k_{\rm out}$); $\omega=\omega_{\rm in}-\omega_{\rm out}$ and $q=k_{\rm in}-k_{\rm out}$ are the energy and momentum transferred along the chain direction, respectively; $|g\rangle$, $|n\rangle$, and $|f\rangle$ are the initial, intermediate, and final states of the RIXS process with energies E_g , E_n , and E_f , respectively; $D_k=\sum_{i,\sigma}e^{ikR_i}D_{i,\sigma}$ is the dipole operator describing the $2p\to 3d$ ($D_{i,\sigma}=\sum_{\alpha}\tilde{c}_{i,\sigma}p_{i,\alpha}^{\dagger}$) and $1s\to 2p$ ($D_{i,\sigma}=[\tilde{c}_{i+1,\sigma}-\tilde{c}_{i,\sigma}]s_{i,\sigma}^{\dagger}$) transition [28,29], where $p_{i,\alpha}^{\dagger}$ and $s_{i,\sigma}^{\dagger}$ are creation operators on the 2p and 1s core levels, respectively; and Γ_n is the core-hole broadening related to the inverse core-hole lifetime. For our numerical calculations we use $\Gamma_n=0.3$ eV (Cu L_3 edge) and 0.15 eV (O K edge) for all n [22,52]. Figures 2(c) and 2(d) show the calculated spectra, which capture the two- and four-spinon excitations at both edges.

The RIXS spectra at the Cu L_3 edge have contributions from both the NSC and SC channels [9,18] while the O K edge has contributions from only the SC channel. To demonstrate this, Figs. 3(a) and 3(b) show the spin-resolved contributions to the Cu L_3 -edge RIXS intensity from the NSC and SC channels, respectively, highlighting the features outside the two-spinon phase space. Figure 3(c) shows the computed intensity profiles of the two channels for momentum transfers along the chain, obtained by integrating the spectral weight along the energy axis within the region enclosed by the red dashed lines in Figs. 3(a) and 3(b). The profiles have been normalized to their maximum values in the probed portion of the Brillouin zone for comparison. From Figs. 3(a) and 3(c), it is clear that the four-spinon excitations in the NSC channel have the maximum spectral weight close to the upper boundary of the two-spinon continuum and a negligible weight at the zone center. Conversely, the four-spinon excitations observed in the SC channel have maximal spectral weight close to $q_{\parallel} = 0$. In Fig. 3(d), we show the experimental Cu L_3 -edge RIXS intensity profile from the same region [see Fig. 2(b) and SM Fig. S2 for the full map [42]]. The experimental profile can be well described by a sum of the NSC and SC channel profiles (in a ratio $\sim 1:1.92$) and a linear background. Our results show that both NSC and SC four-spinons have significant weight outside the two-spinon phase space when probed using Cu L_3 -edge RIXS. This result also explains why the spectral weight distribution in this region of phase space is substantially different from that at the O K edge, where only SC excitations are allowed.

While the KH formalism captures the spectral weight distribution of both the two- and four-spinon excitations, it is desirable to identify the correlation functions leading to these excitations using the UCL expansion [9,23,53]. For a half-filled antiferromagnetic d^9 cuprate, the zeroth-order terms in

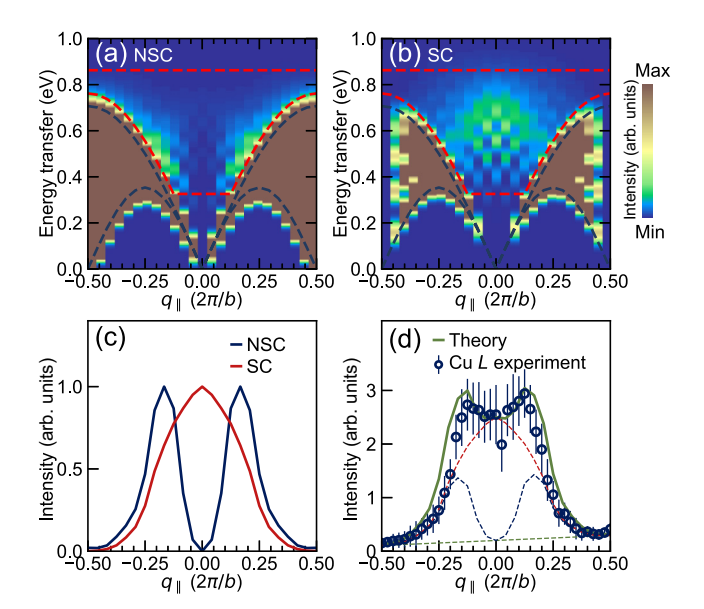


FIG. 3. The calculated Cu L_3 -edge RIXS spectra in the (a) NSC and (b) SC channels, computed using the Kramers-Heisenberg formalism. The brown color represents the maximum spectral weight in the color scale. (c) The normalized intensity profiles of the two spin channels obtained by integrating the region marked by the red dashed lines in (b) and (c). (d) The integrated intensity profile for the same region obtained from the Cu L_3 -edge RIXS experiment on SrCuO₂. The continuous line is a weighted sum of the NSC and SC channel profiles shown in (c) and a linear background to match the experimental profile (see text).

the expansion of the SC and NSC channels are elastic scattering and the conventional dynamical spin structure factor $S(q, \omega)$, respectively [9,42,54]. Corrections to these terms are provided by the higher-order terms in the UCL expansion. For a 1D HAFM, the next generalized correlation functions appearing in the NSC and SC channels are shown in Fig. 4. The kth-order terms in the UCL expansion are

$$S_{(\mathrm{N})\mathrm{SC}}^k(q,\omega) = \sum_{f} \left| \langle f | O_{q,k}^{(\mathrm{N})\mathrm{SC}} | g \rangle \right|^2 \delta(E_f - E_g - \omega),$$

where $O_{q,k}^{(N)SC} = \frac{1}{\sqrt{N}} \sum_i e^{iqR_i} O_{i,k}^{(N)SC}$, and $O_{i,k}^{NSC} = S_i^z [\mathbf{S}_i \cdot (\mathbf{S}_{i+1} + \mathbf{S}_{i-1})]^k$ and $O_{i,k}^{SC} = [\mathbf{S}_i \cdot (\mathbf{S}_{i+1} + \mathbf{S}_{i-1})]^k$ are the effective operators in each channel. Figures 4(a) and 4(b) demonstrate that the spectral weight of the k=1 terms of the SC and NSC channels remains confined to the two-spinon phase space [48,55]. Additional spectral weight only appears outside the two-spinon phase space at second order [Figs. 4(c) and 4(d)]. In other words, the four-spinon excitations seen in the Cu L_3 -edge RIXS experiment are not captured by the first-order nearest-neighbor correlation functions and represent higher-order longer-range spin-spin correlations (see SM [42]).

In conclusion, we have demonstrated that both O Kand Cu L_3 -edge RIXS can probe four-spinon excitations
outside the two-spinon phase space in the 1D HAFM system SrCuO₂. We further showed that these four-spinon
excitations encode information about long-range spin-spin
correlations due to the lifetime of the intermediate state's core

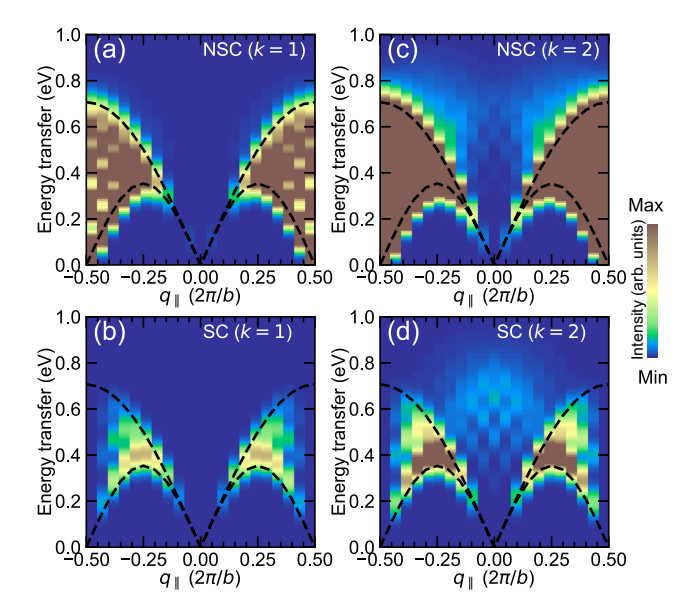


FIG. 4. The generalized dynamical structure factors $S_{(N)SC}^k(q,\omega)$ appearing in higher-order terms of the UCL expansion. (a) and (b) show the intensity maps of the first-order (k=1) terms in the NSC and SC channels, respectively. (c) and (d) show the intensity maps of the second-order (k=2) terms in the NSC and SC channels, respectively. The brown color represents the maximum spectral weight in the color scale.

hole. Higher-order terms in the UCL expansion of the SC channel were explored previously in the context of twomagnon excitations in Cu K-edge RIXS studies of twodimensional cuprates [53,56]. But the relevance of these terms for Cu L_3 -edge RIXS has not been widely explored [9]. We find that terms up to the second order in the UCL expansion are needed to achieve even a qualitative description of the four-spinon excitations at the Cu L_3 edge. Our work illustrates that the Cu L₃-edge RIXS is more sensitive to long-range quantum spin fluctuations in low-dimensional quantum magnets than previously reported. In particular, the NSC channel at this edge probes different long-range correlation functions, which one can exploit for exploring higher-order many-body spin dynamics in a wide range of systems irrespective of their dimensionality or spin degrees of freedom. Additionally, the correlation functions without the explicit core-hole terms can be computed using a number of techniques such as the Bethe ansatz [55], continuous unitary transformation method [57], and quantum Monte Carlo, which can grant access to larger system sizes than ED and reveal other insights about quantum magnets.

U.K. acknowledges support from U.S. DOE NNSA under Contract No. 89233218CNA000001 through the LDRD Program. S.J. acknowledges support from the National Science Foundation under Grant No. DMR-1842056. T.S. was supported by the Swiss National Science Foundation (SNSF) through the SNSF Research Grants No. 200021_178867 and No. 200021L_141325. We acknowledge Diamond Light Source for providing the beamtime on I21 beamline under Proposal No. NR21184. We acknowledge T. Rice for the

technical support throughout the beamtime. We also thank G. B. G. Stenning and D. W. Nye for help on the Laue instru-

ment in the Materials Characterisation Laboratory at the ISIS Neutron and Muon Source.

- [1] D. Scalapino, Phys. Rep. 250, 329 (1995).
- [2] A. Chubukov, D. Pines, and J. Schmalian, A spin fluctuation model for *d*-wave superconductivity, in *The Physics of Superconductors*, edited by K. H. Bennemann and J. B. Ketterson (Springer, Berlin, 2003), Vol. I, pp. 495–590.
- [3] J. Orenstein and A. J. Millis, Science 288, 468 (2000).
- [4] Y. Sidis, S. Pailhès, B. Keimer, P. Bourges, C. Ulrich, and L. P. Regnault, Phys. Status Solidi B 241, 1204 (2004).
- [5] D. J. Scalapino, Rev. Mod. Phys. 84, 1383 (2012).
- [6] P. A. Lee, N. Nagaosa, and X.-G. Wen, Rev. Mod. Phys. 78, 17 (2006).
- [7] N. S. Headings, S. M. Hayden, R. Coldea, and T. G. Perring, Phys. Rev. Lett. 105, 247001 (2010).
- [8] L. J. P. Ament, M. van Veenendaal, T. P. Devereaux, J. P. Hill, and J. van den Brink, Rev. Mod. Phys. 83, 705 (2011).
- [9] C. Jia, K. Wohlfeld, Y. Wang, B. Moritz, and T. P. Devereaux, Phys. Rev. X 6, 021020 (2016).
- [10] L. Braicovich, J. van den Brink, V. Bisogni, M. M. Sala, L. J. P. Ament, N. B. Brookes, G. M. De Luca, M. Salluzzo, T. Schmitt, V. N. Strocov, and G. Ghiringhelli, Phys. Rev. Lett. 104, 077002 (2010).
- [11] M. Minola, G. Dellea, H. Gretarsson, Y. Y. Peng, Y. Lu, J. Porras, T. Loew, F. Yakhou, N. B. Brookes, Y. B. Huang, J. Pelliciari, T. Schmitt, G. Ghiringhelli, B. Keimer, L. Braicovich, and M. Le Tacon, Phys. Rev. Lett. 114, 217003 (2015).
- [12] M. Le Tacon, G. Ghiringhelli, J. Chaloupka, M. M. Sala, V. Hinkov, M. W. Haverkort, M. Minola, M. Bakr, K. J. Zhou, S. Blanco-Canosa, C. Monney, Y. T. Song, G. L. Sun, C. T. Lin, G. M. De Luca, M. Salluzzo, G. Khaliullin, T. Schmitt, L. Braicovich, and B. Keimer, Nat. Phys. 7, 725 (2011).
- [13] M. P. M. Dean, R. S. Springell, C. Monney, K. J. Zhou, J. Pereiro, I. Božović, B. Dalla Piazza, H. M. Rønnow, E. Morenzoni, J. van den Brink, T. Schmitt, and J. P. Hill, Nat. Mater. 11, 850 (2012).
- [14] J. Kim, D. Casa, M. H. Upton, T. Gog, Y.-J. Kim, J. F. Mitchell, M. van Veenendaal, M. Daghofer, J. van den Brink, G. Khaliullin, and B. J. Kim, Phys. Rev. Lett. 108, 177003 (2012).
- [15] Y. Lu, D. Betto, K. Fürsich, H. Suzuki, H.-H. Kim, G. Cristiani, G. Logvenov, N. B. Brookes, E. Benckiser, M. W. Haverkort, G. Khaliullin, M. Le Tacon, M. Minola, and B. Keimer, Phys. Rev. X 8, 031014 (2018).
- [16] H. C. Robarts, M. García-Fernández, J. Li, A. Nag, A. C. Walters, N. E. Headings, S. M. Hayden, and K.-J. Zhou, Phys. Rev. B 103, 224427 (2021).
- [17] A. Nag, H. C. Robarts, F. Wenzel, J. Li, H. Elnaggar, R.-P. Wang, A. C. Walters, M. García-Fernández, F. M. F. de Groot, M. W. Haverkort, and K.-J. Zhou, Phys. Rev. Lett. 124, 067202 (2020).
- [18] L. J. P. Ament, G. Ghiringhelli, M. M. Sala, L. Braicovich, and J. van den Brink, Phys. Rev. Lett. 103, 117003 (2009).
- [19] F. Gel'mukhanov, M. Odelius, S. P. Polyutov, A. Föhlisch, and V. Kimberg, Rev. Mod. Phys. 93, 035001 (2021).
- [20] J. Pelliciari, S. Karakuzu, Q. Song, R. Arpaia, A. Nag, M. Rossi, J. Li, T. Yu, X. Chen, R. Peng, M. García-Fernández, A. C.

- Walters, Q. Wang, J. Zhao, G. Ghiringhelli, D. Feng, T. A. Maier, K.-J. Zhou, S. Johnston, and R. Comin, Nat. Commun. 12, 3122 (2021).
- [21] R. Y. Umetsu, H. Fujiwara, K. Nagai, Y. Nakatani, M. Kawada, A. Sekiyama, F. Kuroda, H. Fujii, T. Oguchi, Y. Harada, J. Miyawaki, and S. Suga, Phys. Rev. B 99, 134414 (2019).
- [22] C. J. Jia, E. A. Nowadnick, K. Wohlfeld, Y. F. Kung, C. C. Chen, S. Johnston, T. Tohyama, B. Moritz, and T. P. Devereaux, Nat. Commun. 5, 3314 (2014).
- [23] L. J. P. Ament, F. Forte, and J. van den Brink, Phys. Rev. B 75, 115118 (2007).
- [24] D. Betto, R. Fumagalli, L. Martinelli, M. Rossi, R. Piombo, K. Yoshimi, D. Di Castro, E. Di Gennaro, A. Sambri, D. Bonn, G. A. Sawatzky, L. Braicovich, N. B. Brookes, J. Lorenzana, and G. Ghiringhelli, Phys. Rev. B 103, L140409 (2021).
- [25] R. Fumagalli, L. Braicovich, M. Minola, Y. Y. Peng, K. Kummer, D. Betto, M. Rossi, E. Lefrançois, C. Morawe, M. Salluzzo, H. Suzuki, F. Yakhou, M. Le Tacon, B. Keimer, N. B. Brookes, M. M. Sala, and G. Ghiringhelli, Phys. Rev. B 99, 134517 (2019).
- [26] J. Schlappa, K. Wohlfeld, K. J. Zhou, M. Mourigal, M. W. Haverkort, V. N. Strocov, L. Hozoi, C. Monney, S. Nishimoto, S. Singh, A. Revcolevschi, J.-S. Caux, L. Patthey, H. M. Ronnow, J. van den Brink, and T. Schmitt, Nature (London) 485, 82 (2012).
- [27] K. Wohlfeld, S. Nishimoto, M. W. Haverkort, and J. van den Brink, Phys. Rev. B 88, 195138 (2013).
- [28] J. Schlappa, U. Kumar, K. J. Zhou, S. Singh, M. Mourigal, V. N. Strocov, A. Revcolevschi, L. Patthey, H. M. Rønnow, S. Johnston, and T. Schmitt, Nat. Commun. 9, 5394 (2018).
- [29] U. Kumar, A. Nocera, E. Dagotto, and S. Johnston, New J. Phys. 20, 073019 (2018).
- [30] B. H. Kim and J. van den Brink, Phys. Rev. B 92, 081105(R) (2015).
- [31] A. Nag, A. Nocera, S. Agrestini, M. Garcia-Fernandez, A. C. Walters, S.-W. Cheong, S. Johnston, and K.-J. Zhou, Nat. Commun. 13, 2327 (2022).
- [32] M. Enderle, B. Fåk, H.-J. Mikeska, R. K. Kremer, A. Prokofiev, and W. Assmus, Phys. Rev. Lett. 104, 237207 (2010).
- [33] L. S. Wu, W. J. Gannon, I. A. Zaliznyak, A. M. Tsvelik, M. Brockmann, J.-S. Caux, M. S. Kim, Y. Qiu, J. R. D. Copley, G. Ehlers, A. Podlesnyak, and M. C. Aronson, Science 352, 1206 (2016).
- [34] M. Mourigal, M. Enderle, A. Klopperpieper, J.-S. Caux, A. Stunault, and H. M. Ronnow, Nat. Phys. 9, 435 (2013).
- [35] B. Lake, D. A. Tennant, J.-S. Caux, T. Barthel, U. Schollwöck, S. E. Nagler, and C. D. Frost, Phys. Rev. Lett. 111, 137205 (2013).
- [36] I. A. Zaliznyak, H. Woo, T. G. Perring, C. L. Broholm, C. D. Frost, and H. Takagi, Phys. Rev. Lett. 93, 087202 (2004).
- [37] N. Motoyama, H. Eisaki, and S. Uchida, Phys. Rev. Lett. 76, 3212 (1996).

- [38] C. Kim, A. Y. Matsuura, Z.-X. Shen, N. Motoyama, H. Eisaki, S. Uchida, T. Tohyama, and S. Maekawa, Phys. Rev. Lett. 77, 4054 (1996).
- [39] B. J. Kim, H. Koh, E. Rotenberg, S.-J. Oh, H. Eisaki, N. Motoyama, S. Uchida, T. Tohyama, S. Maekawa, Z.-X. Shen, and C. Kim, Nat. Phys. 2, 397 (2006).
- [40] M. Knupfer, R. Neudert, M. Kielwein, S. Haffner, M. S. Golden, J. Fink, C. Kim, Z.-X. Shen, M. Merz, N. Nücker, S. Schuppler, N. Motoyama, H. Eisaki, S. Uchida, Z. Hu, M. Domke, and G. Kaindl, Phys. Rev. B 55, R7291 (1997).
- [41] I. A. Zaliznyak, C. Broholm, M. Kibune, M. Nohara, and H. Takagi, Phys. Rev. Lett. 83, 5370 (1999).
- [42] See Supplemental Material at http://link.aps.org/supplemental/ 10.1103/PhysRevB.106.L060406 for O *K*-, Cu *L*₃-edge XAS, Cu *L*₃-edge full RIXS map, and theoretical details, which includes Refs. [9,23,28,48,53,55,58–61].
- [43] https://www.diamond.ac.uk/Instruments/Magnetic-Materials/I21.html.
- [44] M. Karbach, G. Müller, A. H. Bougourzi, A. Fledderjohann, and K.-H. Mütter, Phys. Rev. B 55, 12510 (1997).
- [45] J.-S. Caux and R. Hagemans, J. Stat. Mech.: Theory Exp. (2006) P12013.
- [46] R. Fumagalli, J. Heverhagen, D. Betto, R. Arpaia, M. Rossi, D. Di Castro, N. B. Brookes, M. Moretti Sala, M. Daghofer, L. Braicovich, K. Wohlfeld, and G. Ghiringhelli, Phys. Rev. B 101, 205117 (2020).
- [47] V. Bisogni, S. Kourtis, C. Monney, K. Zhou, R. Kraus, C. Sekar, V. Strocov, B. Büchner, J. van den Brink, L. Braicovich, T. Schmitt, M. Daghofer, and J. Geck, Phys. Rev. Lett. 112, 147401 (2014).

- [48] F. Forte, M. Cuoco, C. Noce, and J. van den Brink, Phys. Rev. B 83, 245133 (2011).
- [49] A. Nocera, U. Kumar, N. Kaushal, G. Alvarez, E. Dagotto, and S. Johnston, Sci. Rep. 8, 11080 (2018).
- [50] A. C. Walters, T. G. Perring, J.-S. Caux, A. T. Savici, G. D. Gu, C.-C. Lee, W. Ku, and I. A. Zaliznyak, Nat. Phys. 5, 867 (2009).
- [51] S. Li, A. Nocera, U. Kumar, and S. Johnston, Commun. Phys. 4, 217 (2021).
- [52] W. S. Lee, S. Johnston, B. Moritz, J. Lee, M. Yi, K. J. Zhou, T. Schmitt, L. Patthey, V. Strocov, K. Kudo, Y. Koike, J. van den Brink, T. P. Devereaux, and Z. X. Shen, Phys. Rev. Lett. 110, 265502 (2013).
- [53] F. Forte, L. J. P. Ament, and J. van den Brink, Phys. Rev. B 77, 134428 (2008).
- [54] U. Kumar, A. Nocera, E. Dagotto, and S. Johnston, Phys. Rev. B 99, 205130 (2019).
- [55] A. Klauser, J. Mossel, J.-S. Caux, and J. van den Brink, Phys. Rev. Lett. 106, 157205 (2011).
- [56] J. P. Hill, G. Blumberg, Y.-J. Kim, D. S. Ellis, S. Wakimoto, R. J. Birgeneau, S. Komiya, Y. Ando, B. Liang, R. L. Greene, D. Casa, and T. Gog, Phys. Rev. Lett. 100, 097001 (2008).
- [57] G. Ferkinghoff, L. Müller, G. S. Uhrig, U. Kumar, and B. Fauseweh, arXiv:2012.01513.
- [58] L. J. P. Ament, Ph.D. thesis, Universiteit Leiden, Netherlands, 2010
- [59] Y. Lu and M. W. Haverkort, Phys. Rev. Lett. 119, 256401 (2017).
- [60] S. Kourtis, J. van den Brink, and M. Daghofer, Phys. Rev. B 85, 064423 (2012).
- [61] J.-I. Igarashi and T. Nagao, Phys. Rev. B 85, 064422 (2012).